f_2, as shown in Figure 3.37(b). The magnitudes of the envelope detector outputs following the two filters are proportional to $|H_1(f)|$ and $|H_2(f)|$. Subtracting these two outputs yields the overall characteristic

$$H(f) = |H_1(f)| - |H_2(f)| \tag{3.163}$$

as shown in Figure 3.37(c). The combination is approximately linear over a wider frequency range than would be the case for either filter used alone, and it is clearly possible to make $H(f_c) = 0$.

Several techniques can be used to combine the outputs of two envelope detectors. A differential amplifier can be used, for example. Another alternative, using a strictly passive circuit, is shown in Figure 3.37(d). A center-tapped transformer supplies the input signal $x_c(t)$ to the inputs of the two bandpass filters. The center frequencies of the two bandpass filters are given by

$$f_i = \frac{1}{2\pi\sqrt{L_i C_i}} \tag{3.164}$$

for $i = 1, 2$. The envelope detectors are formed by the diodes and the resistor-capacitor combinations $R_e C_e$. The output of the upper envelope detector is proportional to $|H_1(f)|$, and the output of the lower envelope detector is proportional to $|H_2(f)|$. The output of the upper envelope detector is the positive portion of its input envelope, and the output of the lower envelope detector is the negative portion of its input envelope. Thus $y_D(t)$ is proportional to $|H_1(f)| - |H_2(f)|$. This system is known as a *balanced discriminator* because the response to the undeviated carrier is balanced so that the net response is zero.

3.3 INTERFERENCE

We now consider the effect of interference in communication systems. In real-world systems interference occurs from various sources, such as radio frequency emissions from transmitters having carrier frequencies close to that of the carrier being demodulated. We also study interference because the analysis of systems in the presence of interference provides us with important insights into the behavior of systems operating in the presence of noise, which is the topic of Chapter 6. In this section we consider both linear modulation and angle modulation. It is important to understand the very different manner in which these two systems behave in the presence of interference.

3.3.1 Interference in Linear Modulation

As a simple case of linear modulation in the presence of interference, we consider the received signal having the spectrum (single-sided) shown in Figure 3.38. The received

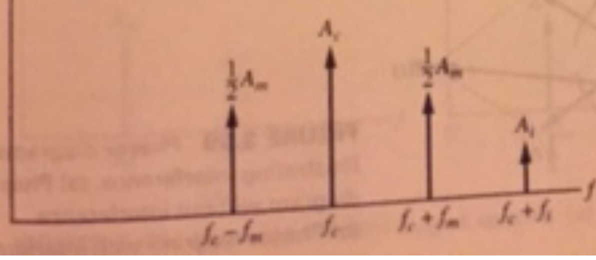

FIGURE 3.38 Assumed received-signal spectrum.

signal consists of three components: a carrier component, a pair of sidebands representing a sinusoidal message signal, and an undesired interfering tone of frequency $f_c + f_i$. The input to the demodulator is therefore

$$x_c(t) = A_c \cos \omega_c t + A_i \cos(\omega_c + \omega_i)t + A_m \cos \omega_m t \cos \omega_c t \tag{3.165}$$

Multiplying $x_c(t)$ by $2 \cos \omega_c t$ and lowpass-filtering (coherent demodulation) yields

$$y_D(t) = A_m \cos \omega_m t + A_i \cos \omega_i t \tag{3.166}$$

where we have assumed that the interference component is passed by the filter and that the dc term resulting from the carrier is blocked. From this simple example we see that the signal and interference are additive at the receiver output if the interference is additive at the receiver input. This result was obtained because the coherent demodulator operates as a linear demodulator.

The effect of interference with envelope detection is quite different because of the nonlinear nature of the envelope detector. The analysis with envelope detection is much more difficult than the coherent demodulation case. Some insight can be gained by writing $x_c(t)$ in a form that leads to the phasor diagram. In order to develop the phasor diagram we write (3.165) in the form

$$x_c(t) = \mathrm{Re}\left[A_c e^{j\omega_c t} + A_i e^{j\omega_c t} e^{j\omega_i t} + \frac{1}{2} A_m e^{j\omega_c t} e^{j\omega_m t} + \frac{1}{2} A_m e^{j\omega_c t} e^{-j\omega_m t}\right] \tag{3.167}$$

which can be written as

$$x_r(t) = \mathrm{Re}\left\{e^{j\omega_c t}\left[A_c + A_i e^{j\omega_i t} + \frac{1}{2} A_m e^{j\omega_m t} + \frac{1}{2} A_m e^{-j\omega_m t}\right]\right\} \tag{3.168}$$

The phasor diagram is constructed with respect to the carrier by taking the carrier frequency as equal to zero. The phasor diagrams are illustrated in Figure 3.39, both with and without interference. The output of an ideal envelope detector is $R(t)$ in both cases. The phasor diagrams illustrate that interference induces both an amplitude distortion and a phase deviation.

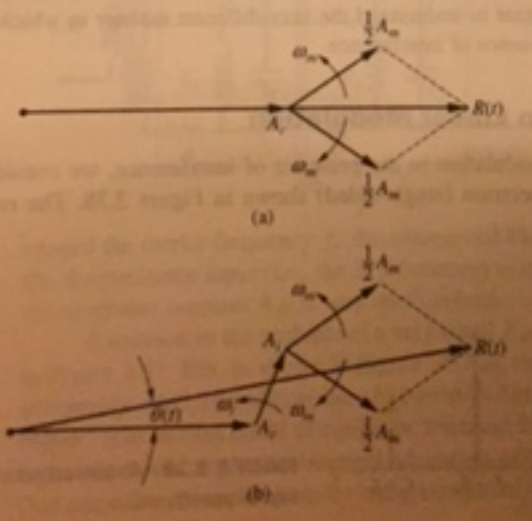

FIGURE 3.39 Phasor diagra[m] illustrating interference. (a) Ph[asor] diagram without interference. (b) Phasor diagram with interfe[rence]

The effect of interference with envelope detection is determined by writing (3.165) as

$$\begin{aligned} x_r(t) &= A_c \cos \omega_c t + A_m \cos \omega_m t \cos \omega_c t \\ &\quad + A_i [\cos \omega_c t \cos \omega_i t - \sin \omega_c t \sin \omega_i t] \end{aligned} \tag{3.169}$$

which is

$$x_r(t) = [A_c + A_m \cos \omega_m t + A_i \cos \omega_i t] \cos \omega_c t - A_i \sin \omega_i t \sin \omega_c t \tag{3.170}$$

If $A_c \gg A_i$, which is the usual case of interest, the second term in (3.170) is negligible compared to the first term. For this case, the output of the envelope detector is

$$y_D(t) \cong A_m \cos \omega_m t + A_i \cos \omega_i t \tag{3.171}$$

assuming that the dc term is blocked. Thus, for the small interference case, envelope detection and coherent demodulation are essentially equivalent.

If $A_c \ll A_i$, the assumption cannot be made that the second term of (3.170) is negligible, and the output is significantly different. To show this, (3.165) is rewritten as

$$\begin{aligned} x_r(t) &= A_c \cos(\omega_c + \omega_i - \omega_i)t + A_i \cos(\omega_c + \omega_i)t \\ &\quad + A_m \cos \omega_m t \cos(\omega_c + \omega_i - \omega_i)t \end{aligned} \tag{3.172}$$

which, when we use appropriate trigonometric identities, becomes

$$\begin{aligned} x_r(t) = {} & A_c [\cos(\omega_c + \omega_i)t \cos \omega_i t + \sin(\omega_c + \omega_i)t \sin \omega_i t] \\ & + A_i \cos(\omega_c + \omega_i)t \\ & + A_m \cos \omega_m t [\cos(\omega_c + \omega_i)t \cos \omega_i t + \sin(\omega_c + \omega_i)t \sin \omega_i t] \end{aligned} \tag{3.173}$$

Equation (3.173) can also be written as

$$\begin{aligned} x_r(t) &= [A_i + A_c \cos \omega_i t + A_m \cos \omega_m t \cos \omega_i t] \cos(\omega_c + \omega_i)t \\ &\quad + [A_c \sin \omega_i t + A_m \cos \omega_m t \sin \omega_i t] \sin(\omega_c + \omega_i)t \end{aligned} \tag{3.174}$$

If $A_i \gg A_c$, the second term in (3.174) is negligible with respect to the first term. It follows that the envelope detector output is approximated by

$$y_D(t) \cong A_c \cos \omega_i t + A_m \cos \omega_m t \cos \omega_i t \tag{3.175}$$

At this point, several observations are in order. In envelope detectors, the largest high-frequency component is treated as the carrier. If $A_c \gg A_i$, the effective demodulation carrier has a frequency ω_c, whereas if $A_i \gg A_c$, the *effective* carrier frequency becomes the interference frequency $\omega_c + \omega_i$.

The spectra of the envelope detector output are illustrated in Figure 3.40 for $A_c \gg A_i$, and for $A_c \ll A_i$. For $A_c \gg A_i$ the interfering tone simply appears as a sinusoidal component, having frequency f_i at the output of the envelope detector. This illustrates that

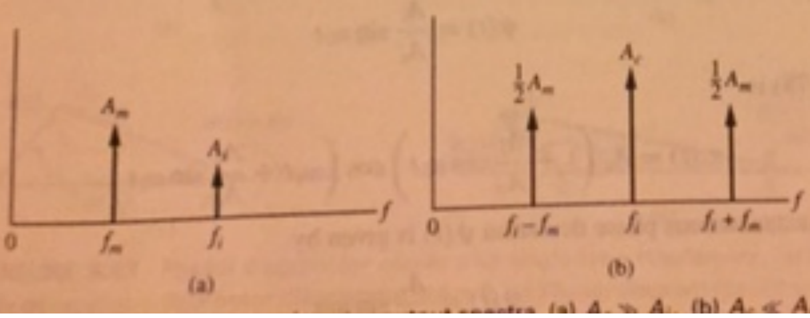

...put spectra. (a) $A_c \gg A_i$. (b) $A_c \ll A_i$.

for $A_c \gg A_i$, the envelope detector performs as a linear demodulator. The situation is much different for $A_c \ll A_i$, as can be seen from (3.175) and Figure 3.40(b). For this case we see that the sinusoidal message signal, having frequency f_m, modulates the interference tone. The output of the envelope detector has a spectrum that reminds us of the spectrum of an AM signal with carrier frequency f_m and sideband components at $f_i + f_m$ and $f_i - f_m$. The message signal is effectively lost. This degradation of the desired signal is called the *threshold effect* and is a consequence of the nonlinear nature of the envelope detector. We will study the threshold effort in detail in Chapter 6 when we investigate the effect of noise in analog systems.

3.3.2 Interference in Angle Modulation

We now consider the effect of interference in angle modulation. We will see that the effect of interference in angle modulation is quite different from what was observed in linear modulation. Furthermore, we will see that the effect of interference in an FM system can be reduced by placing a lowpass filter at the discriminator output. We will consider this problem in considerable detail since the results will provide significant insight into the behavior of FM discriminators operating in the presence of noise.

Assume that the input to a PM or FM ideal discriminator is an unmodulated carrier plus an interfering tone at frequency $\omega_c + \omega_i$. Thus the input to the discriminator is assumed to have the form

$$x_r(t) = A_c \cos \omega_c t + A_i \cos(\omega_c + \omega_i)t \tag{3.176}$$

which can be written as

$$x_r(t) = A_c \cos \omega_c t + A_i \cos \omega_i t \cos \omega_c t - A_i \sin \omega_i \sin \omega_c t \tag{3.177}$$

Using Equations (3.50) through (3.54), the preceding expression can be written as

$$x_r(t) = R(t) \cos [\omega_c t + \psi(t)] \tag{3.178}$$

where

$$R(t) = \sqrt{(A_c + A_i \cos \omega_i t)^2 + (A_i \sin \omega_i t)^2} \tag{3.179}$$

and

$$\psi(t) = \tan^{-1} \frac{A_i \sin \omega_i t}{A_c + A_i \cos \omega_i t}$$

If $A_c \gg A_i$, Equations (3.179) and (3.180) can be approximated as

$$R(t) = A_c + A_i \cos \omega_i t \tag{3.181}$$

and

$$\psi(t) = \frac{A_i}{A_c} \sin \omega_i t \tag{3.182}$$

Thus (3.178) is

$$x_r(t) = A_c \left(1 + \frac{A_i}{A_c} \cos \omega_i t\right) \cos \left(\omega_c t + \frac{A_i}{A_c} \sin \omega_i t\right) \tag{3.183}$$

since the instantaneous phase deviation $\psi(t)$ is given by

$$\psi(t) = \frac{A_i}{A_c} \sin \omega_i t \tag{3.184}$$

the ideal discriminator output for PM is

$$y_D(t) = K_D \frac{A_i}{A_c} \sin \omega_i t \tag{3.185}$$

and for FM is

$$\begin{aligned} y_D(t) &= \frac{1}{2\pi} K_D \frac{d}{dt} \frac{A_i}{A_c} \sin \omega_i t \\ &= K_D \frac{A_i}{A_c} f_i \cos \omega_i t \end{aligned} \tag{3.186}$$

For both cases, the discriminator output is a sinusoid of frequency f_i. The amplitude of the discriminator output, however, is proportional to the frequency f_i for the FM case. It can be seen that for small f_i, the interfering tone has less effect on the FM system than on the PM system and that the opposite is true for large values of f_i. Values of $f_i > W$, the bandwidth of $m(t)$, are of little interest, since they can be removed by a lowpass filter following the discriminator.

For larger values of A_i the assumption that $A_i \ll A_c$ cannot be made and (3.186) no longer can describe the discriminator output. If the condition $A_i \ll A_c$ does not hold, the discriminator is not operating above threshold and the analysis becomes much more difficult. Some insight into this case can be obtained from the phasor diagram, which is obtained by writing (3.176) in the form

$$x_r(t) = \text{Re}\,\{[A_c + A_i e^{j\omega_i t}]e^{j\omega_c t}\} \tag{3.187}$$

The term in square brackets defines the phasor. The phasor diagram is shown in Figure 3.41(a). The carrier phase is taken as the reference and the interference phase is

$$\theta(t) = \omega_i t \tag{3.188}$$

Approximations to the phase of the resultant $\psi(t)$ can be determined using the phasor diagram.

From Figure 3.41(b) we see that the magnitude of the discriminator output will be small when $\theta(t)$ is near zero. This results because for $\theta(t)$ near zero, a given change in $\theta(t)$ will result in a much smaller change in $\psi(t)$. Using the relationship between arc length, s, angle, θ, and radius, r, which is $s = \theta r$, we obtain

$$s = \theta(t)\, A_i \approx (A_c + A_i)\psi(t), \quad \theta(t) \approx 0 \tag{3.189}$$

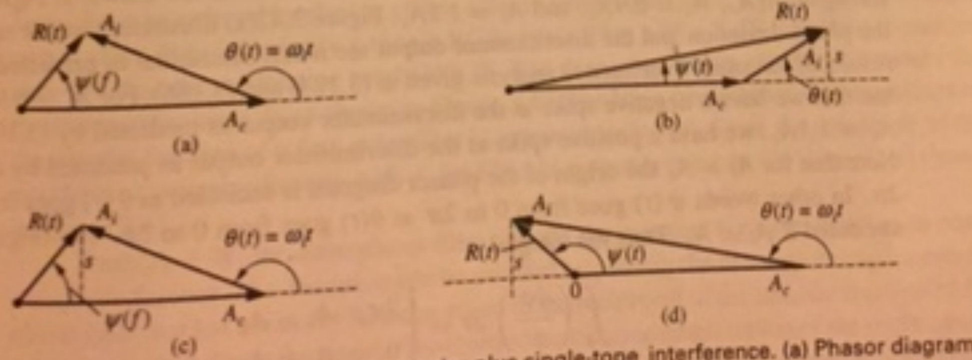

FIGURE 3.41 Phasor diagram for carrier plus single-tone interference. (a) Phasor diagram for general $\theta(t)$. (b) Phasor diagram for $\theta(t) \approx 0$. (c) Phasor diagram for $\theta(t) \approx \pi$ and $A_i \lesssim A_c$. (d) Phasor diagram for $\theta(t) \approx \pi$ and $A_i \gtrsim A_c$.

Solving for $\psi(t)$ yields

$$\psi(t) \approx \frac{A_i}{A_c + A_i}\omega_i t \tag{3.190}$$

Since the discriminator output is defined by

$$y_D(t) = \frac{K_D}{2\pi}\frac{d\psi}{dt} \tag{3.191}$$

we have

$$y_D(t) = K_D \frac{A_i}{A_c + A_i} f_i, \quad \theta(t) \approx 0 \tag{3.192}$$

This is a positive quantity for $f_i > 0$ and a negative quantity for $f_i < 0$.

If A_i is slightly less than A_c, denoted $A_i \lesssim A_c$ and $\theta(t)$ is near π, a small positive change in $\theta(t)$ will result in a large negative change in $\psi(t)$. The result will be a negative spike appearing at the discriminator output. From Figure 3.41(c) we can write

$$s = A_i(\pi - \theta(t)) \approx (A_c - A_i)\psi(t), \quad \theta(t) \approx \pi \tag{3.193}$$

which can be expressed as

$$\psi(t) \approx \frac{A_i(\pi - \omega_i t)}{A_c - A_i} \tag{3.194}$$

Using (3.191) we see that the discriminator output is

$$y_D(t) = -K_D \frac{A_i}{A_c - A_i} f_i, \quad \theta(t) \approx \pi \tag{3.195}$$

This is a negative quantity for $f_i > 0$ and a positive quantity for $f_i < 0$.

If A_i is slightly greater than A_c, denoted $A_i \gtrsim A_c$, and $\theta(t)$ is near π, a small positive change in $\theta(t)$ will result in a large positive change in $\psi(t)$. The result will be a positive spike appearing at the discriminator output. From Figure 3.41(d) we can write

$$s = A_i[\pi - \theta(t)] \approx (A_i - A_c)[\pi - \psi(t)], \quad \theta(t) \approx \pi \tag{3.196}$$

Solving for $\psi(t)$ and differentiating gives the discriminator output

$$y_D(t) \approx K_D \frac{A_i}{A_i - A_c} f_i \tag{3.197}$$

Note that this is a positive quantity for $f_i > 0$ and a negative quantity for $f_i < 0$.

The phase deviation and discriminator output waveforms are shown in Figure 3.42 for $A_i = 0.1A_c$, $A_i = 0.9A_c$, and $A_i = 1.1A_c$. Figure 3.42(a) illustrates that for small A_i the phase deviation and the discriminator output are nearly sinusoidal as predicted by the results of the small interference analysis given in (3.184) and (3.186). For $A_i = 0.9A_c$, we see that we have a negative spike at the discriminator output as predicted by (3.195). For $A_c = 1.1A_c$, we have a positive spike at the discriminator output as predicted by (3.197). Note that for $A_i > A_c$ the origin of the phasor diagram is encircled as $\theta(t)$ goes from 0 to 2π. In other words $\psi(t)$ goes from 0 to 2π as $\theta(t)$ goes from 0 to 2π. The origin is not encircled if $A_i < A_c$. Thus the integral

$$\int_T \left(\frac{d\psi}{dt}\right) dt = \begin{cases} 2\pi, & A_i > A_c \\ 0, & A_i < A_c \end{cases} \tag{3.198}$$

where T is the time required for $\theta(t)$ to go from $\theta(t) = 0$ to $\theta(t) = 2\pi$. In other words $T = 2\pi/\omega_i$. Thus the area under the discriminator output curve is 0 for parts (a) and (b)

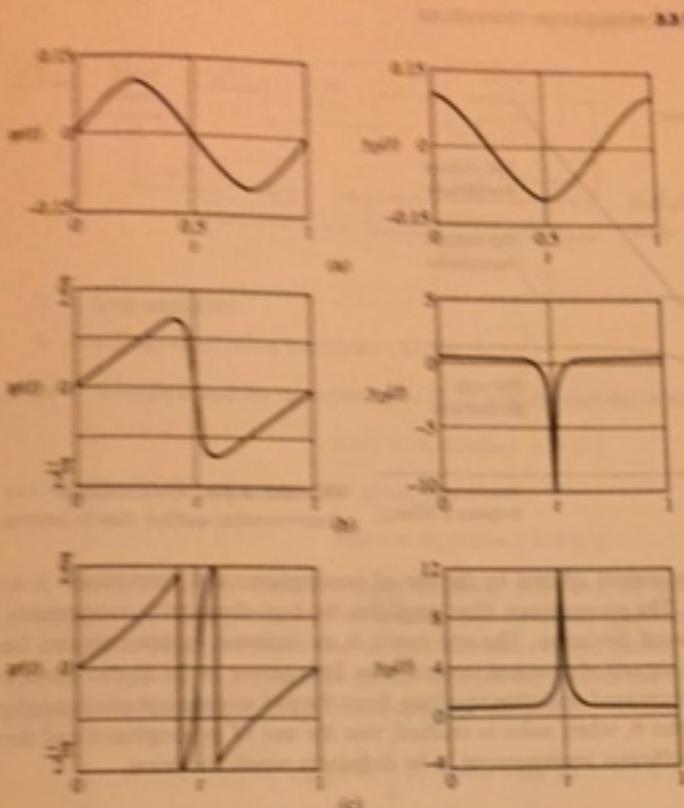

FIGURE 3.42 Phase deviation and discriminator outputs due to interference. (a) Phase deviation and discriminator output for $A_i = 0.2A_c$. (b) Phase deviation and discriminator output for $A_i = 0.9A_c$. (c) Phase deviation and discriminator output for $A_i = 1.1A_c$.

of Figure 3.42 and $2\pi K_D$ for the discriminator output curve in Figure 3.42(c). The origin encirclement phenomenon will be revisited in Chapter 6 when demodulation of FM signals in the presence of noise is examined. An understanding of the interference results presented here will provide valuable insights when noise effects are considered.

For operation above threshold $A_i \ll A_c$, the severe effect of interference on FM for large f_i can be reduced by placing a filter, called a *deemphasis filter*, at the FM discriminator output. This filter is typically a simple RC lowpass filter with a 3-dB frequency considerably less than the modulation bandwidth W. The deemphasis filter effectively reduces the interference for large f_i, as shown in Figure 3.43. For large frequencies, the magnitude of the transfer function of a first-order filter is approximately $1/f$. Since the amplitude of the interference increases linearly with f_i for FM, the output is constant for large f_i, as shown in Figure 3.43.

Since $f_3 < W$, the deemphasis filter distorts the message signal in addition to combating interference. The distortion can be avoided by passing the message through a *preemphasis filter* that has a transfer function equal to the reciprocal of the transfer function of the deemphasis filter. Since the transfer function of the cascade combination of the preemphasis and deemphasis filters is unity, there is no detrimental effect on the modulation. This yields the system shown in Figure 3.44.

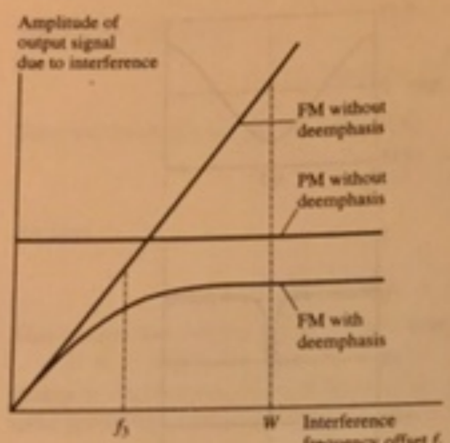

FIGURE 3.43 Amplitude of discriminator output due to interference.

The improvement offered by the use of preemphasis and deemphasis is not gained without a price. The preemphasis filter amplifies the high-frequency components, and this results in increased deviation. The end result is an increase in transmission bandwidth. However, many signals of practical interest have little power in the higher-frequency components, so the increased deviation resulting from the use of preemphasis is negligible. We will see in Chapter 6, when noise is studied, that the use of preemphasis and deemphasis often provides sufficient improvement to be definitely worth the price.

3.4 FEEDBACK DEMODULATORS

We have already studied the technique of FM to AM conversion for demodulating an angle-modulated signal. We will see in Chapter 6 that improved performance in the of noise can be gained by utilizing a feedback demodulator. In this section we the basic operation of several types of feedback demodulators. Such systems used in today's communication systems not only because of their superior but also because of their ease of implementation using inexpensive integrated phase-locked loop is the basic building block.

3.4.1 Phase-Locked Loops for FM Demodulation

A block diagram of a phase-locked loop (PLL) is shown in Figure 3.45. Such generally contains four basic elements:

1. A phase detector
2. A loop filter